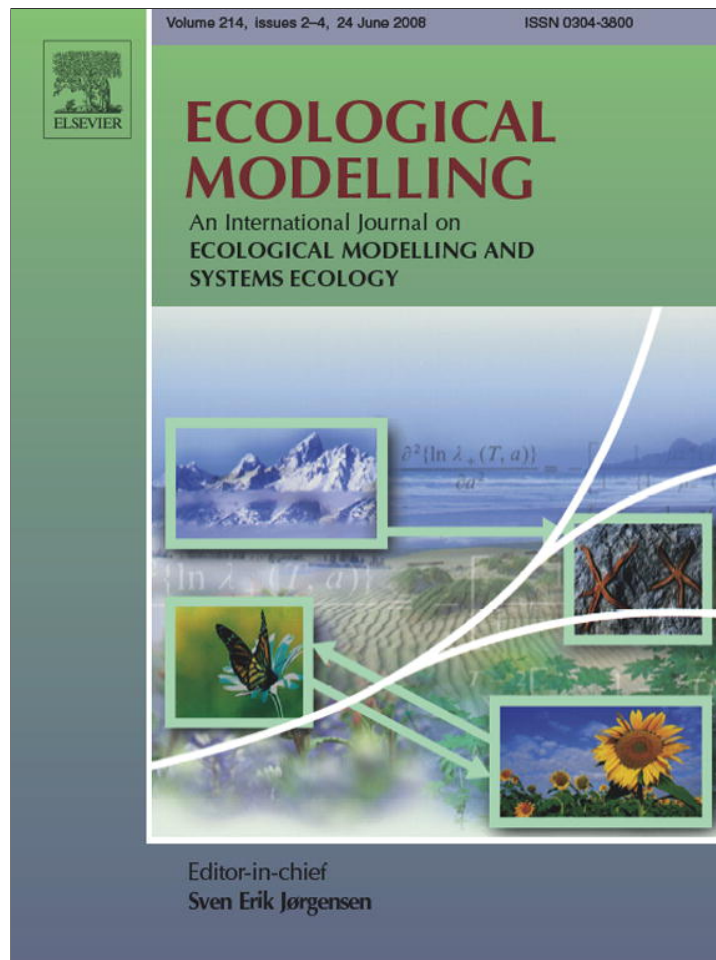


Provided for non-commercial research and education use.  
Not for reproduction, distribution or commercial use.



This article appeared in a journal published by Elsevier. The attached copy is furnished to the author for internal non-commercial research and education use, including for instruction at the authors institution and sharing with colleagues.

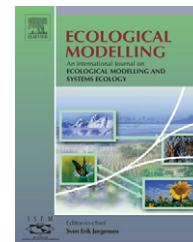
Other uses, including reproduction and distribution, or selling or licensing copies, or posting to personal, institutional or third party websites are prohibited.

In most cases authors are permitted to post their version of the article (e.g. in Word or Tex form) to their personal website or institutional repository. Authors requiring further information regarding Elsevier's archiving and manuscript policies are encouraged to visit:

<http://www.elsevier.com/copyright>



ELSEVIER

available at [www.sciencedirect.com](http://www.sciencedirect.com)journal homepage: [www.elsevier.com/locate/ecolmodel](http://www.elsevier.com/locate/ecolmodel)

## Multiyear heterotrophic soil respiration: Evaluation of a coupled CO<sub>2</sub> transport and carbon turnover model

M. Herbst<sup>a,\*</sup>, H.J. Hellebrand<sup>b</sup>, J. Bauer<sup>a</sup>, J.A. Huisman<sup>a</sup>, J. Šimůnek<sup>c</sup>,  
L. Weihermüller<sup>a</sup>, A. Graf<sup>a</sup>, J. Vanderborght<sup>a</sup>, H. Vereecken<sup>a</sup>

<sup>a</sup> Agrosphere, ICG-4, Forschungszentrum Jülich GmbH, D-52428 Jülich, Germany

<sup>b</sup> Leibnitz-Institut für Agrartechnik Bornim e.V., Max-Eyth-Allee 100, D-14469 Potsdam, Germany

<sup>c</sup> Department of Environmental Sciences, University of California, Riverside, CA 92521, USA

### ARTICLE INFO

#### Article history:

Received 31 July 2007

Received in revised form

29 January 2008

Accepted 15 February 2008

Published on line 28 March 2008

#### Keywords:

Soil organic carbon

Heterotrophic soil respiration

Model

Soilco2

RothC

### ABSTRACT

Modelling of soil respiration plays an important role in the prediction of climate change. Soil respiration is usually divided in a fraction originating from root respiration and a heterotrophic fraction originating from microbial decomposition of soil organic carbon. This paper reports on the coupling of an one-dimensional water, heat and CO<sub>2</sub> flux model (SOILCO2) with a pool concept of carbon turnover (RothC) for the prediction of soil heterotrophic respiration. In order to test this coupled model, it was applied to a bare soil experimental plot located in Bornim, Germany. Soil temperature and soil water content measurements were used for comparison with the respective model predictions. An 8 years data set of CO<sub>2</sub> efflux measurements, covering a broad range of atmospheric conditions, was used to evaluate the model. In a first step we quantified the improvement of the CO<sub>2</sub> efflux prediction due to the coupling of the flux model with a pool concept of carbon turnover. The humus pool decomposition rate constant and its soil water content dependent reduction were derived from the first 5 years of CO<sub>2</sub> efflux measurements using inverse modelling. The following 3 years of measurements were used to validate the model. The overall model performance of CO<sub>2</sub> efflux predictions was acceptable with the measured and simulated mean daily respiration being 0.861 and 0.868 g C m<sup>-2</sup> d<sup>-1</sup>, respectively, and a mean absolute difference between modelled and measured rates of 0.21 g C m<sup>-2</sup> d<sup>-1</sup>. The inverse estimation of the humus decomposition rate constant resulted in a value of 0.04 year<sup>-1</sup>, which is higher than the default value in RothC. This is attributed to the agricultural practice during the experiment.

© 2008 Elsevier B.V. All rights reserved.

## 1. Introduction

Soil respiration, as a part of the carbon cycle, is one key factor in the prediction of climate change (IPCC, 2007; Smith et al., 2003; Davidson and Janssens, 2006). In this context, the

accurate modelling of soil respiration plays a major role, since models, that are validated for present conditions may be used to predict soil CO<sub>2</sub> efflux under future boundary conditions, like increased temperatures or elevated CO<sub>2</sub> levels. Changes in the soil carbon pools contribute significantly to soil res-

\* Corresponding author. Tel.: +49 2461 618674; fax: +49 2461 612518.

E-mail addresses: [m.herbst@fz-juelich.de](mailto:m.herbst@fz-juelich.de) (M. Herbst), [jhellebrand@atb-potsdam.de](mailto:jhellebrand@atb-potsdam.de) (H.J. Hellebrand), [j.bauer@fz-juelich.de](mailto:j.bauer@fz-juelich.de) (J. Bauer), [s.huisman@fz-juelich.de](mailto:s.huisman@fz-juelich.de) (J.A. Huisman), [jiri.simunek@ucr.edu](mailto:jiri.simunek@ucr.edu) (J. Šimůnek), [l.weihermueller@fz-juelich.de](mailto:l.weihermueller@fz-juelich.de) (L. Weihermüller), [a.graf@fz-juelich.de](mailto:a.graf@fz-juelich.de) (A. Graf), [j.vanderborght@fz-juelich.de](mailto:j.vanderborght@fz-juelich.de) (J. Vanderborght), [h.vereecken@fz-juelich.de](mailto:h.vereecken@fz-juelich.de) (H. Vereecken).

0304-3800/\$ – see front matter © 2008 Elsevier B.V. All rights reserved.

doi:10.1016/j.ecolmodel.2008.02.007

piration. These changes, in combination with shifts in plant carbon fixation, determine ecosystem carbon storage below-ground and its exchange with the atmosphere (Paustian et al., 2000). Small changes in the soil carbon stocks have a considerable impact on the atmospheric CO<sub>2</sub> at the global scale (Eliasson et al., 2005), since soil organic matter contains about twice as much carbon as the earth's atmosphere. A good understanding of the influence of soil water content and temperature on the microbially mediated release of CO<sub>2</sub> from soil carbon stocks is crucial for an accurate prediction of climate effects on global carbon cycling (Fang and Moncrieff, 2001; Zak et al., 1999). A global increase in decomposition rates due to increased temperatures could cause the release of more soil carbon. However, if the soil temperature increase coincides with drier soil conditions, the increase could be dampened (Zak et al., 1999). Thus, a sound estimation of soil respiration as a function of soil temperature and water content is crucial to the understanding of global climate change.

Existing models to predict soil respiration can be divided in two categories that differ in temporal scale and methodology. On the other hand, models like SOILCO<sub>2</sub> (Šimůnek and Suarez, 1993), the model of Cook et al. (1998) or the model of Pumpanen et al. (2003) were developed to estimate the soil CO<sub>2</sub> efflux at the scale of hours to days. These models focus on a physically based description of CO<sub>2</sub> transport in the soil. Typically, these models treat the CO<sub>2</sub> production in a simplified way by using an optimum respiration rate as a source term constant in time and/or space (Šimůnek and Suarez, 1993; Pumpanen et al., 2003). On the other hand, carbon turnover models like RothC (Coleman and Jenkinson, 2005), CENTURY (Parton et al., 1994) or CANDY (Franko et al., 1997) usually operate at the temporal scale of months to decades using pool concepts to account for microbiological carbon decomposition (Smith et al., 1997). RothC, like all other carbon turnover models, assumes that CO<sub>2</sub> production by microbial decomposition is immediately rejected to the atmosphere. Further, the carbon turnover models are mostly bulk models based on a conceptual approach (Smith et al., 1997; Molina and Smith, 1998). Although these models account for the influence of the abiotic factors soil temperature and soil water content on carbon decomposition (Smith et al., 2003), they do not resolve these variables over the depth of a soil profile. Usually soil organic matter is partitioned into at least two pools or compartments, characterised by different decomposition rate constants. Typically, the models in this category lack a feedback mechanism between local CO<sub>2</sub> concentration in the soil profile and microbial CO<sub>2</sub> production from carbon decomposition, although it should be noted that some of the CO<sub>2</sub> transport models of the first category also neglect this (Suwa et al., 2004; Hashimoto and Komatsu, 2006).

The availability of combined CO<sub>2</sub> transport and carbon turnover models is still limited. To our knowledge, there are three models that use a pool concept of carbon turnover in combination with a CO<sub>2</sub> transport module. One is PATCIS (Fang and Moncrieff, 1999), which applies a two-pool carbon concept but is focussed on forest ecosystems and requires soil water content and temperature as input. Another one is PASTIS (Cannavo et al., 2006), which applies a combined C and N biotransformation module (Garnier et al., 2003). The third one is the model of Jassal et al. (2004), which applies a

two-pool carbon turnover concept with a CO<sub>2</sub> transport model very similar to the model of Šimůnek and Suarez (1993). In this paper, we coupled a model of water flux, heat and CO<sub>2</sub> transport (SOILCO<sub>2</sub>, Šimůnek and Suarez, 1993) with the pool concept of a well-known and state-of-the-art carbon turnover model (RothC-26.3, Coleman and Jenkinson, 2005) to allow for a closed soil carbon balancing and a holistic description of soil carbon cycling and respiration. We envision that the use of a carbon pool model leads to a better description of the CO<sub>2</sub> production and the dynamics of the soil carbon stocks, whereas the use of a flow and transport model improves the description of the soil state variables, which in turn determine the rate constants in the pool model. In contrast to the three 'coupled' models mentioned above, the coupled SOILCO<sub>2</sub>/RothC model has the advantage of using an established concept with pools, that are measurable (Falloon et al., 1998; Skjemstad et al., 2004; Zimmermann et al., 2007) and for which rate constants and environmental correction factors are documented. To test the coupled model of CO<sub>2</sub> transport and carbon turnover, the predictions for heterotrophic soil respiration are compared to respiration measurements made with a closed chamber system on a bare soil plot. The aims were to (i) test the coupled model concept and to validate the model for the prediction of CO<sub>2</sub> efflux; (ii) improve our understanding of the influence of soil water content and temperature on microbial CO<sub>2</sub> production under field conditions; and (iii) estimate the decomposition rate constants of the recalcitrant carbon pools by model inversion with measurements of CO<sub>2</sub> efflux.

It should be noted that soil respiration is usually divided in a fraction originating from root respiration (autotrophic) and another fraction originating from microbial decomposition of soil organic carbon (heterotrophic). For long-term averages, the heterotrophic fraction is almost as large as the autotrophic fraction and contributes significantly to the production of CO<sub>2</sub> by soils (Akinremi et al., 1999; Smith et al., 2003; Saiz et al., 2006). Unfortunately, it is cumbersome to separate root respiration from CO<sub>2</sub> originating from microbial activity in an experimental way (Trumbore, 2006; Scott-Denton et al., 2006). In this study, the focus is on heterotrophic respiration. Future studies should also consider root respiration and its interaction with environmental variables.

## 2. Materials and methods

### 2.1. Soil water, heat and CO<sub>2</sub> flux

SOILCO<sub>2</sub> (Šimůnek and Suarez, 1993) is a physically based one-dimensional model for soil water and heat flux as well as for CO<sub>2</sub> transport. Since the original approaches of SOILCO<sub>2</sub> for water, heat and CO<sub>2</sub> flux in the water and gas phase were not modified in the coupled model, we describe them only briefly. The unsaturated soil water flux is described by the Richards equation:

$$\frac{\partial \theta}{\partial h} \frac{\partial h}{\partial t} = \frac{\partial}{\partial z} \left[ k(h) \left( \frac{\partial h}{\partial z} - 1 \right) \right] - Q \quad (1)$$

where  $t$  is the time [T],  $z$  is the vertical coordinate [L],  $\theta$  is the volumetric water content [L<sup>3</sup>L<sup>-3</sup>],  $h$  is the pressure head [L],  $k$  is the unsaturated hydraulic conductivity [L T<sup>-1</sup>] and  $Q$

is a source/sink term [ $T^{-1}$ ]. The soil water capacity  $\partial\theta/\partial h$  and the unsaturated hydraulic conductivity function  $k(h)$  are calculated according to Van Genuchten (1980). Soil heat transport is described by:

$$C_p(\theta) \frac{\partial T}{\partial t} = \frac{\partial}{\partial z} \left[ \lambda(\theta) \frac{\partial T}{\partial z} \right] - C_w q_w \frac{\partial T}{\partial z} \quad (2)$$

where  $T$  is the soil temperature [K],  $\lambda$  is the apparent thermal conductivity [ $W L^{-1} K^{-1}$ ],  $C_p$  is the volumetric heat capacity of the porous medium [ $J L^{-3} K^{-1}$ ],  $C_w$  is the volumetric heat capacity of the soil water [ $J L^{-3} K^{-1}$ ] and  $q_w$  is the water flux [ $L T^{-1}$ ].

Transport of  $CO_2$  is simulated by considering diffusion  $J_{da}$  [ $L T^{-1}$ ] and convection  $J_{ca}$  [ $L T^{-1}$ ] in the gas phase, as well as dispersion  $J_{dw}$  [ $L T^{-1}$ ] and convection  $J_{cw}$  [ $L T^{-1}$ ] of  $CO_2$  dissolved in the liquid phase:

$$\frac{\partial c_T}{\partial t} = - \frac{\partial}{\partial z} (J_{da} + J_{dw} + J_{ca} + J_{cw}) + S \quad (3)$$

where  $c_T$  [ $L^3 L^{-3}$ ] is the total volumetric concentration of  $CO_2$  and  $S$  [ $L^3 L^{-3} T^{-1}$ ] is the production term of  $CO_2$ . The concentration of  $CO_2$  in the liquid phase is assumed to be in instantaneous equilibrium with the gas phase concentration. The predominant transport process for  $CO_2$  is the diffusion in the gas phase, calculated according to

$$J_{da} = -\theta_a D_a \frac{\partial c_a}{\partial z} \quad (4)$$

where  $\theta_a$  is the volumetric air content [ $L^3 L^{-3}$ ],  $c_a$  is the volumetric  $CO_2$  concentration in the gas phase [ $L^3 L^{-3}$ ] and  $D_a$  is the effective soil matrix diffusion coefficient of  $CO_2$  in the gas phase [ $L^2 T^{-1}$ ]. This effective diffusion coefficient accounts for the tortuosity of the pore space and is calculated by the Millington–Quirk approach:

$$D_a = D_{as} \frac{\theta_a^{7/3}}{\theta_s} \quad (5)$$

where  $D_{as}$  is the diffusion coefficient of  $CO_2$  in free air [ $L^2 T^{-1}$ ] and  $\theta_s$  is the saturated water content [ $L^3 L^{-3}$ ]. The estimation of the  $CO_2$  transport caused by air advection in the soil is based on a piston gas flow assumption, which implies that any water volume change in the soil profile must be immediately matched by a corresponding change in gas volume:

$$q_a(z) = q_w(0) - q_w(z) + \int_z^{L_r} Q(z) dz \quad (6)$$

where  $q_a$  is the soil air flux [ $L T^{-1}$ ] and  $L_r$  is the length of the soil profile [ $L$ ]. For a more detailed description of the  $CO_2$  transport processes the reader is referred to the work of Šimůnek and Suarez (1993).

## 2.2. Production of $CO_2$

In the original version of the SOILCO2 model the total source term of  $CO_2$  production  $S$  [ $L^3 L^{-3} T^{-1}$ ] is the sum of the production by soil micro-organisms  $\gamma_S$  [ $L^3 L^{-3} T^{-1}$ ] and plant

roots  $\gamma_P$  [ $L^3 L^{-3} T^{-1}$ ]:

$$S = \gamma_S + \gamma_P \quad (7)$$

The value of  $\gamma_S$  in the original SOILCO2 is calculated from an optimal  $CO_2$  production rate  $\gamma_{S0}$  [ $L^3 L^{-2} T^{-1}$ ], which is constant in time and distributed with an exponential function over the profile depth:

$$\gamma_S(z) = \gamma_{S0} a e^{-a(L_r - z)} \quad (8)$$

where  $L_r$  is the profile depth [ $L$ ]. The exponential function is scaled with the constant  $a$  to ensure that the function is normalized according to the depth of the soil profile.

For the modified version of SOILCO2, the pool concept of the carbon turnover model RothC-26.3 (Coleman and Jenkinson, 2005) is used to estimate the  $CO_2$  production by soil micro-organisms. It is assumed that soil organic matter (SOM) is composed of a variety of organic compounds, which are characterised by different decomposition rates. C-pools group substances with decomposition rates of the same order of magnitude. In the RothC model, SOM is partitioned into five compartments, where the inert organic matter pool (IOM) [ $ML^{-3}$ ] is resistant to decomposition. The other four compartments are actively decomposed. These are the decomposable plant material (DPM) [ $ML^{-3}$ ], the resistant plant material (RPM) [ $ML^{-3}$ ], the microbial biomass (BIO) [ $ML^{-3}$ ] and the humified organic matter (HUM) [ $ML^{-3}$ ]. Incoming plant carbon is partitioned between DPM and RPM. Both DPM and RPM decompose to form  $CO_2$ , BIO and HUM. The partitioning between  $CO_2$ , BIO and HUM depends on the clay content of the soil using the following equation:

$$b = \frac{CO_2}{BIO + HUM} = 1.67 (1.85 + 1.6 e^{-0.0786 \text{ clay}^{100}}) \quad (9)$$

where the clay fraction [ $MM^{-1}$ ] is expressed on a gravimetric basis. The fraction of  $CO_2$  carbon  $x_{CO_2}$  is thus equal to  $b/(b+1)$ . Both BIO and HUM decompose to generate more  $CO_2$ , BIO and HUM. The ratio  $CO_2/(BIO + HUM)$  for the decomposition of BIO and HUM is the same as for the decomposition of DPM and RPM. The decomposition process is assumed to follow first-order kinetics:

$$\frac{\partial C_x}{\partial t} = C_x (-\lambda_x \prod_j f_j) \quad (10)$$

where the change of the concentration of any soil organic matter pool  $C_x$  [ $ML^{-3}$ ] with time is characterised by the respective optimum decomposition rate  $\lambda_x$  [ $T^{-1}$ ], which is scaled with the product of the reduction factors  $f_w$  for pressure head,  $f_T$  for temperature and  $f_{CO_2}$  for  $CO_2$  concentration:

$$\prod_j f_j = f_T f_w f_{CO_2} \quad (11)$$

For the decomposition of DPM and RPM, Eq. (10) can be extended by the input from plant material  $C_{P_{inp}}$  [ $ML^{-3}$ ]. This

can be written in the discrete form as:

$$C_{p,i} = (C_{p,i-1} + y_{inp,x} C_{P_{inp},i-1}) e^{-\lambda \prod_j f_j \Delta t} \quad (12)$$

where  $C_p$  is the concentration of the pool [ $ML^{-3}$ ], the index  $p$  loops over the fast pools DPM and RPM and  $y_{inp,x} = 0.59$  for  $x = \text{DPM}$  and  $0.41$  for  $x = \text{RPM}$  (Coleman and Jenkinson, 2005),  $i$  is the index for the time increment and  $\Delta t$  is the length of the time step [T]. The incoming carbon from plant material  $P_{in}$  [ $ML^{-2}$ ] is distributed evenly across the soil up to a given depth  $D_p$  [L] to calculate the carbon input from plant material:

$$C_{P_{inp}} = \frac{P_{in}}{D_p} \quad (13)$$

Thus, the concentration of the decomposed carbon from DPM and RPM  $d_p$  [ $ML^{-3}$ ] is equal to:

$$d_{p,i} = (C_{p,i-1} + y_{inp} C_{P_{inp},i-1}) [1 - e^{-\lambda \prod_j f_j \Delta t}] \quad (14)$$

The BIO and the HUM pool are charged by all active pools:

$$C_{s,i} = C_{s,i-1} e^{-\lambda \prod_j f_j \Delta t} + x_p \sum_{r=1}^4 d_{r,i} \quad (15)$$

where  $x_p$  is equal to  $(1 - x_{CO_2}) \times 0.45$  and  $(1 - x_{CO_2}) \times 0.54$  for BIO and HUM, respectively. Here, index  $s$  loops over the BIO and HUM pool, and index  $r$  loops over the four pools DPM, RPM, BIO and HUM. The concentration of the decomposed carbon from BIO and HUM  $d_s$  is equal to:

$$d_{s,i} = C_{s,i-1} [1 - e^{-\lambda \prod_j f_j \Delta t}] \quad (16)$$

Thus, the total mass concentration of  $CO_2$  carbon [ $ML^{-3}$ ] equals the sum of the  $CO_2$  carbon produced from DPM, RPM, BIO and HUM:

$$C_{CO_2C,i} = x_{CO_2} \sum_{r=1}^4 d_{r,i} \quad (17)$$

The  $CO_2$  mass concentration  $C_{CO_2}$  [ $ML^{-3}$ ] is calculated from the  $CO_2$  carbon mass concentration  $C_{CO_2C}$  [ $ML^{-3}$ ] by scaling with the ratio between the molecular mass of  $CO_2$  and C, which is  $0.044 \text{ kg mol}^{-1} / 0.012 \text{ kg mol}^{-1}$ . The  $CO_2$  mass concentration is converted into a volumetric concentration assuming an ideal gas:

$$V_{CO_2} = \frac{C_{CO_2} RT}{M_{CO_2} P} \quad (18)$$

where  $V_{CO_2}$  is the volumetric  $CO_2$  concentration [ $L^3 L^{-3}$ ],  $R$  is the universal gas constant ( $=6.2 \times 10^{14} \text{ kg cm}^2 \text{ d}^{-2} \text{ K}^{-1} \text{ mol}^{-1}$ ) [ $ML^2 T^{-2} K^{-1} n^{-1}$ ],  $T$  is the absolute temperature [K],  $M_{CO_2}$  is the molar mass of  $CO_2$  ( $=0.044 \text{ kg mol}^{-1}$ ) [ $M n^{-1}$ ], and  $P$  is the atmospheric pressure ( $=7.6 \times 10^{12} \text{ kg cm}^{-1} \text{ d}^{-2}$ ) [ $ML^{-1} T^{-2}$ ]. The  $CO_2$  production rate, which replaces the  $\gamma_s$  of the original approach in Eq. (7), is calculated according to

$$\gamma_s = \frac{V_{CO_2}}{\Delta t} \quad (19)$$

The reduction of the  $CO_2$  production as a function of the  $CO_2$  concentration is based on Michaelis–Menten kinetics (Šimůnek and Suarez, 1993). The original SOILCO2 approach was slightly modified in order to obtain a value of 1.0 for optimum conditions:

$$f_{CO_2}(c_a) = \frac{0.21 - c_a}{0.42 - c_a - K_M^*} + 1 - \frac{0.21}{0.42 - K_M^*} \quad \text{for } c_a < 0.21 \quad (20)$$

$$f_{CO_2}(c_a) = 0.0 \quad \text{for } c_a \geq 0.21$$

where  $c_a$  is the  $CO_2$  concentration [ $LL^{-3}$ ] and  $K_M^*$  is the Michaelis' constant for the  $CO_2$  concentration [ $L^3 L^{-3}$ ], which was set to  $0.19 \text{ cm}^3 \text{ cm}^{-3}$ .

The reduction factors for pressure head are calculated according to Šimůnek et al. (1996):

$$f_w(h) = 1.0 \quad \text{for } h_1 \leq h \leq +\infty$$

$$f_w(h) = \frac{\log_{10}|h| - \log_{10}|h_2|}{\log_{10}|h_1| - \log_{10}|h_2|} \quad \text{for } h_2 \leq h < h_1 \quad (21)$$

$$f_w(h) = 0.0 \quad \text{for } -\infty \leq h < h_2$$

where  $h_1$  is the pressure head for optimum conditions [L], and  $h_2$  is the pressure head below which  $CO_2$  production ceases [L]. According to Rodrigo et al. (1997) this functional relation between pressure head and  $CO_2$  production, originally developed by Andrén and Paustian (1987), was frequently applied to describe the influence of soil water availability on microbial activity.

Compared to Šimůnek and Suarez (1993), the original Arrhenius-type temperature reduction function was shifted to obtain values of 1 for the RothC reference temperature  $T_{ref}$  [K] of 282.4 K:

$$f_T(T) = e^{[E(T - T_{ref})/RT_{ref}]} \quad (22)$$

where  $T$  is the absolute temperature [K] and  $E$  is the reaction activation energy [ $ML^2 T^{-2} n^{-1}$ ].

### 2.3. Experimental data

The data was obtained at the experimental plot of the Institute of Agricultural Engineering in Bornim, close to Berlin (Germany). The predominating soil type is an arenosol (Hellebrand et al., 2003), which properties are summarized in Table 1. The bare soil plot, where the  $CO_2$  efflux measurements were carried out, was kept free from plants by grubbing up to a depth of 10 cm whenever a small amount of weeds became visible. Due to this weeding practice small amounts of fresh plant input, mainly root material, were incorporated into the soil at the weeding dates. However, we further simply refer to the plot as a 'bare soil plot', since this is the closest description of the experimental conditions.

Average daily soil temperature at a depth of 20 cm was determined from measurements made between 1 February 1999 and 31 October 2000 (Fig. 1). Soil water content was determined gravimetrically at 12 plots surrounding the bare soil plot by using mixed samples taken from 0 to 30 cm depth from 25 March 2003 to 20 December 2005. The 12 plots were planted with different crops. Mean average soil water content and standard deviation are calculated by bulking the data from

**Table 1 – Properties of the soil genetic horizons: clay fraction (<2  $\mu\text{m}$ ), silt fraction (2–53  $\mu\text{m}$ ), soil organic carbon SOC, bulk density  $\rho_b$  and soil hydraulic properties according to Van Genuchten (1980): saturated water content  $\theta_s$ , residual water content  $\theta_r$ , inverse of the bubbling pressure  $\alpha$ , shape parameter  $n$  and saturated hydraulic conductivity  $K_s$**

Horizon	Depth (cm)	Clay ( $\text{g g}^{-1}$ )	Silt ( $\text{g g}^{-1}$ )	SOC ( $\text{g g}^{-1}$ )	$\rho_b$ ( $\text{g cm}^{-3}$ )	$\theta_s$ ( $\text{cm}^3 \text{cm}^{-3}$ )	$\alpha$ ( $\text{cm}^{-1}$ )	$n$ (–)	$K_s$ ( $\text{cm d}^{-1}$ )
Ap	0–30	0.062	0.159	0.0084	1.35	0.428	0.139	1.42	442.8
Ahl	30–60	0.060	0.183	0.0055	1.45	0.386	0.110	1.44	235.1
Bt	60–82	0.174	0.206	0.0020	1.50	0.350	0.097	1.34	88.0
Cv	82–100	0.122	0.257	0.0010	1.50	0.367	0.084	1.38	86.9

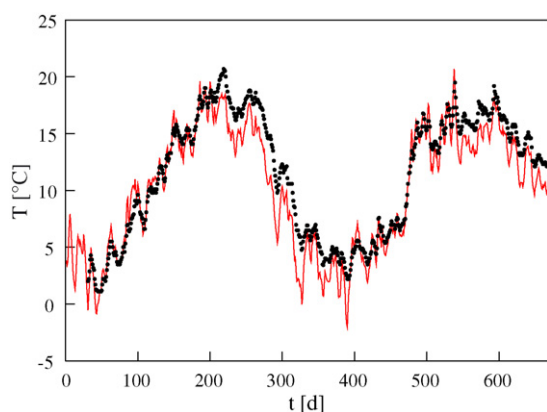


**Fig. 1 – Simulated (red line) and measured (points) soil temperature at 20 cm depth. (For interpretation of the references to colour in this figure legend, the reader is referred to the web version of the article.)**

the 12 plots (Fig. 2). Typically, the plots were sampled every week. Since the plots were cropped, only the measurements outside the vegetation period were considered in the model validation.

From January 1999 until December 2006,  $\text{CO}_2$  effluxes were measured with a closed chamber system and an automated gas chromatograph (GC) approximately every second day (Hellebrand et al., 2005). The gas flux chambers had a volume to area ratio of 0.315 m (volume 0.064  $\text{m}^3$ , diameter 0.509 m).

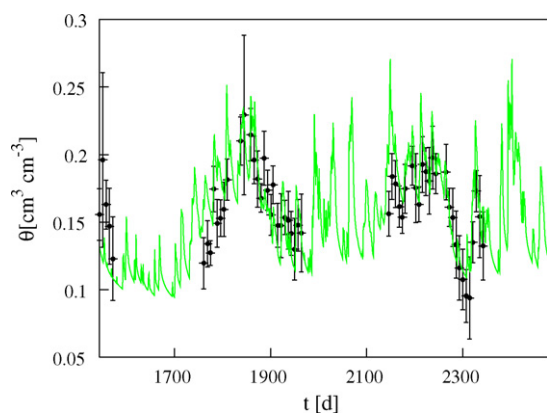


**Fig. 2 – Simulated (green line) and measured average (dots) soil water content (0–30 cm depth), bars indicate standard deviation. (For interpretation of the references to colour in this figure legend, the reader is referred to the web version of the article.)**

Fluxes were measured between 9.00 and 10.00 a.m. Two evacuated gas samplers (100  $\text{cm}^3$  bottles with taps) were connected to each box. The first one was opened when the box was put on the water sealed ring inserted in the soil and the second one after about 1 h enclosure time. The samplers were then connected to the GC injection control system. The GC used an electron capture detector to determine the  $\text{CO}_2$  concentration. The increase in concentration observed for 1 h periods was used to calculate the  $\text{CO}_2$  efflux (Hellebrand et al., 2003). In order to detect erroneous flux measurements, e.g. due to difficulties with air tightness during the sampling procedure, the whole data set was filtered. A moving average of five consecutive measurements was calculated and measurements that were not within the range of the moving average  $\pm$  the standard deviation of the entire data set ( $=0.56 \text{ g C m}^{-2} \text{ d}^{-1}$ ) were discarded (4% of the measurements). During the first 5 years ( $t \leq 1825 \text{ d}$ ), the period for which the model was inverted, 861  $\text{CO}_2$  efflux measurements were available. For the following 3 years (validation period,  $1825 \text{ d} < t < 2920 \text{ d}$ ), 566 measurements were available. Due to the weeding practice small amounts of fresh plant material entered the soil. In order to match the modelled SOC in the top soil with the measured SOC values, it was found that  $177 \text{ g C m}^{-2} \text{ year}^{-1}$  (this is the net primary production) must have entered the soil as fresh plant material. The respiration of this fresh plant material contributed to 43% of the total measured  $\text{CO}_2$  respiration. The amount of fresh plant material was obviously linked to a certain amount of autotrophic respiration, which also contributed to the measured  $\text{CO}_2$  fluxes. Assuming that the autotrophic respiration was 50% of the net primary production of every year (Kirschbaum et al., 2001), which was assumed to be  $177 \text{ g C m}^{-2} \text{ year}^{-1}$ , the autotrophic respiration was 21.5% of the total measured respiration. To ensure that the model inversion for the estimation of the carbon pool decay rates was only based on heterotrophic  $\text{CO}_2$  fluxes, the measured  $\text{CO}_2$  fluxes were reduced by 21.5%.

#### 2.4. Model setup and initialization

The reference evapotranspiration was computed according to the Penman–Monteith approach from daily air temperature, air humidity, wind speed and sunshine duration (Smith et al., 1996). The latter was used to estimate daily net radiation. The meteorological data was measured at the station of the German Weather Service located in Potsdam, approximately 10 km away from the experimental plot in Bornim. The potential reference evapotranspiration was converted into the required potential evaporation (Fig. 3) by scaling with a factor of 0.9 (Penman, 1948).

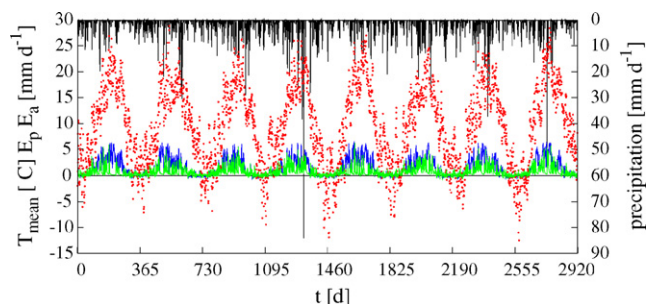


**Fig. 3 – Measured daily precipitation (black surface), measured air temperature at 2 m (red dots), simulated potential evaporation (blue line) and simulated actual evaporation (green line) for the simulation period. (For interpretation of the references to colour in this figure legend, the reader is referred to the web version of the article.)**

The soil hydraulic properties (saturated water content  $\theta_s$  [ $L^3 L^{-3}$ ], inverse of the bubbling pressure  $\alpha$  [ $L^{-1}$ ], shape parameter  $n$  and saturated hydraulic conductivity  $K_s$  [ $L T^{-1}$ ]) were estimated with the pedotransfer functions of Rawls and Brakensiek (1985) from clay content, silt content and bulk density (Table 1). The residual water content  $\theta_r$  was assumed to be zero for all soil horizons. Since no measurements were available, the bulk density was set to standard values increasing with profile depth. Except for the plough horizon, the carbon content of the deeper soil layers was not known and therefore estimated (Table 1).

The initial relative fraction of each carbon pool [ $M M^{-1}$ ] was assumed to be constant with depth (i.e. fraction of IOM is 8% of soil organic carbon for each soil horizon, see Table 2). Since the plot was cleared 2 years before the start of the experiment, it was assumed that no fresh plant material was present anymore. Thus, the RPM and DPM pool were initially set to zero. The IOM fraction was calculated from the total SOC using the pedotransfer function developed by Falloon et al. (1998). After consideration of DPM, RPM and IOM, the remaining soil organic carbon must equal the sum of the HUM and the BIO pool. The relatively small BIO fraction of this sum was determined by assuming a BIO to HUM pool ratio of 0.0272 (Zimmermann et al., 2007). These pool fractions were then used to initialise the model (Table 2).

The upper boundary for the water flow was defined by atmospheric conditions. At the bottom of the profile at 1 m

depth, a Dirichlet boundary ( $h = -200$  cm) was imposed. For heat transport, the air temperature measured at 2 m was used as a time dependent Dirichlet boundary condition at the soil surface. The bottom boundary was set to a constant soil temperature using a Dirichlet boundary condition (Table 3). The atmospheric  $CO_2$  concentration was imposed as a time independent Dirichlet boundary condition at the top of the soil profile, while a no-flux boundary condition was imposed at the bottom for the  $CO_2$  transport. For the discretization in space, we used 100 elements of 1 cm thickness each.

## 2.5. Model inversion

The coupled SOILCO2/RothC model was inverted for the parameter  $h_2$  of the water content reduction function (Eq. (21)) and the decomposition rate constant for the HUM pool  $\lambda_{HUM}$ . The inverse estimation of the HUM decomposition rate constant was necessary because the original rate constant resulted in a rather strong underestimation of the  $CO_2$  efflux. The  $h_2$  parameter was also inverted since it influenced the estimation of  $\lambda_{HUM}$  and was not known a priori. The  $h_2$  parameter slightly affects the temporal course of  $CO_2$  production within a year, whereas  $\lambda_{HUM}$  strongly influences the total amount of  $CO_2$  production. The Nelder–Mead Simplex algorithm (Nelder and Mead, 1965) was used to invert the model. The objective function used in the inversion equally weighted the coefficient of determination between measured and modelled daily  $CO_2$  effluxes and the overall sum of measured and modelled  $CO_2$  efflux. To allow a consistent comparison between the original SOILCO2 model and the coupled model, the SOILCO2 model was inverted for the  $h_2$  parameter and the optimal  $CO_2$  production  $\gamma_{SO}$  in Eq. (8) with the same procedure.

## 2.6. Inversion and validation criteria

For the inversion and validation we used various criteria to quantify the agreement between the measurements and the model predictions. The first criterion was the mean absolute error MAE, which is simply the mean of the absolute residuals. Also a commonly used criterion for model validation is the root mean square error (RMSE), where the root of the mean squared residuals is calculated. MAE and RMSE have the unit of the considered variable. The squared residuals are also used for the second criterion applied, which is the coefficient of model efficiency EF (Nash and Sutcliffe, 1970). Here they are used to determine the proportion of the deviation from the

**Table 2 – Initial RothC pools of the arenosol and pool fractions; biomass carbon BIO, humic fraction HUM, inert organic matter IOM and total soil organic carbon SOC**

Horizon	BIO ( $g C m^{-2}$ )	HUM ( $g C m^{-2}$ )	IOM ( $g C m^{-2}$ )	SOC ( $g C m^{-2}$ )
Ap	84	3050	273	3406
Ahl	59	2138	191	2388
Bt	16	591	53	660
Cv	7	242	22	270
Fraction (%)	2	90	8	100

**Table 3 – Selected model input parameters and initial conditions**

Parameter		Value	Unit
$K_m^*$	Michaelis' constant	0.19	$\text{cm}^3 \text{cm}^{-3}$
$E$	Activation energy	55.5	$\text{kJ mol}^{-1}$
$D_{as}$	Diffusion coefficient of $\text{CO}_2$ in air	13737.6	$\text{cm}^2 \text{d}^{-1}$
$D_{ws}$	Diffusion coefficient of $\text{CO}_2$ in water	1.529	$\text{cm}^2 \text{d}^{-1}$
$\lambda_w$	Dispersivity in water	1.5	cm
$h_1$	Critical pressure head	-70	cm
$h_{ini}$	Initial pressure head	-200	cm
$C_{ini}$	Initial $\text{CO}_2$ concentration	0.001	$\text{cm}^3 \text{cm}^{-3}$
$C_{top}$	$\text{CO}_2$ concentration at soil surface	0.00033	$\text{cm}^3 \text{cm}^{-3}$
$T_{bot}$	Bottom soil temperature	8	$^\circ\text{C}$
$D_p$	Incorporation depth of plant material input	10	cm
$\lambda_T$	Thermal dispersivity	1.5	cm

observed mean, which can be explained by the model:

$$EF = \frac{\sum_{i=1}^n (x_o - \bar{x}_o)_i^2 - \sum_{i=1}^n (x_o - x_s)_i^2}{\sum_{i=1}^n (x_o - \bar{x}_o)_i^2} \quad (23)$$

where  $x_o$  is the observed value at time  $t$ ,  $x_s$  is the simulation result at time  $t$  and  $\bar{x}_o$  is the arithmetic mean of the observed values. The EF is a dimensionless criterion. Values between  $-\infty$  and 1 can be calculated for this index, the latter indicating that observation and model are completely in agreement. The coefficient of determination  $R^2$  is given by

$$R^2 = \left[ \frac{\sum_{i=1}^n (x_o - \bar{x}_o)_i (x_s - \bar{x}_s)_i}{\sqrt{\sum_{i=1}^n (x_o - \bar{x}_o)_i^2 \sum_{i=1}^n (x_s - \bar{x}_s)_i^2}} \right]^2 \quad (24)$$

where  $\bar{x}_s$  is the arithmetic mean of the simulated values. The Index of Agreement IA (Willmott, 1981) was also applied. The

IA is also dimensionless and ranges between 0 and 1:

$$IA = 1 - \frac{\sum_{i=1}^n (x_o - x_s)_i^2}{\sum_{i=1}^n (|x_o - \bar{x}_o| + |x_s - \bar{x}_o|)_i^2} \quad (25)$$

Because  $R^2$ , EF and IA are dimensionless, they can be used to compare the model quality between different variables, while the RMSE gives an idea of the model error in the units of the variable under consideration.

### 3. Results and discussion

#### 3.1. Soil water content and temperature

The comparison between measured and simulated soil temperature at 20 cm depth (Fig. 1) indicates very good agreement ( $R^2 = 0.93$ ,  $n = 639$ ). Slight differences occurred mostly during the second half of the year, at the end of summer and autumn 1999 (time steps 220–350), when the soil temperature was slightly underestimated. The mean absolute error (MAE) was 1.43 K and the root mean square error (RMSE) of 1.76 K was

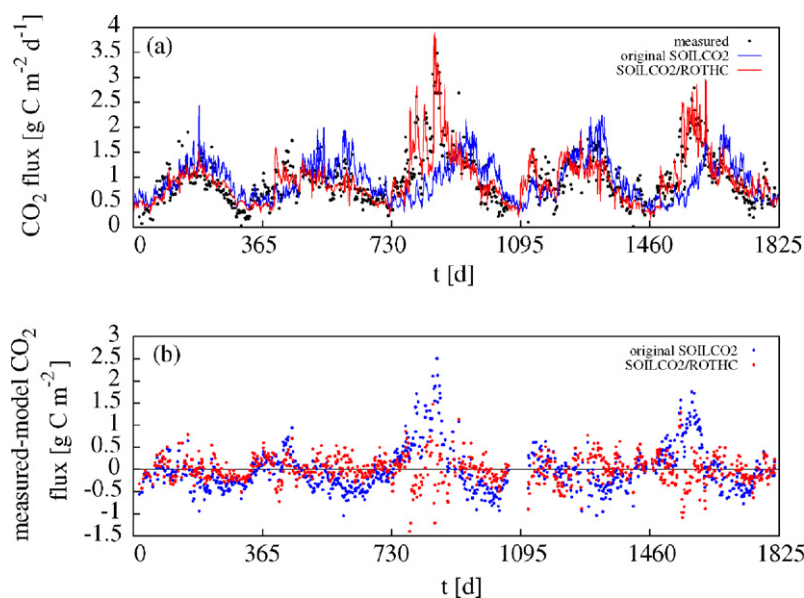


**Fig. 4 – Simulated and measured daily respiration fluxes (a) and residuals between the simulated and measured respiration (b) for the original model and the coupled model version.**

only slightly higher. The measured mean temperature at 20 cm depth during that validation period was 11.4 °C, whereas the model mean was 10.4 °C. This might be the result of the bottom boundary condition, which could have been slightly too low for that period. Even at 1 m depth, there may be some temperature variations over the years which might have caused a small error due to the deviation of the actual 1 m temperature from the long-term average we used as the lower boundary condition.

The soil water content measurements outside the vegetation period were also used for model validation. The modelled mean soil water content of the 0–30 cm soil layer was in good agreement with the weekly measurements (Fig. 2), which is supported by a MAE of 0.021 cm<sup>3</sup> cm<sup>-3</sup>, a RMSE of 0.026 cm<sup>3</sup> cm<sup>-3</sup> and a coefficient of determination of 0.55 (n=57). The mean of the measured soil water content was 0.160 cm<sup>3</sup> cm<sup>-3</sup>, which was slightly overestimated by the model with a predicted mean of 0.167 cm<sup>3</sup> cm<sup>-3</sup>.

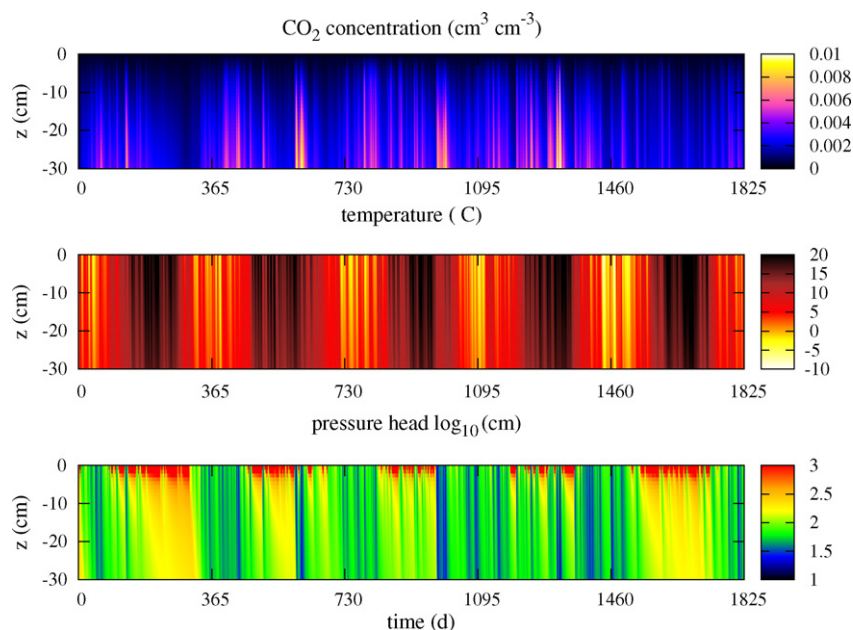
### 3.2. Soil respiration

Fig. 4a presents a comparison between measured and modelled soil respiration of the original SOILCO2 model and the coupled model developed in this study. The original SOILCO2 model underestimates the measured CO<sub>2</sub> effluxes during spring and early summer when fresh plant material entered the topsoil. Fig. 4b shows that the residuals between the measurements and the coupled SOILCO2/RothC are on average closer to zero than for the original SOILCO2. In particular the third and the fifth year of the modelling period show rather large residuals for the original SOILCO2, which is not given to such an extent for the coupled model. The effect of adding fresh plant material on soil respiration cannot be modelled by the original approach using a time-invariant optimum CO<sub>2</sub> production rate of 0.44 cm<sup>3</sup> cm<sup>-2</sup> d<sup>-1</sup>, as determined by the inversion (Eq. (8)). The original SOILCO2 model has a R<sup>2</sup> of 0.18, an IA of 0.64, a MAE of 0.36 gC m<sup>-2</sup> d<sup>-1</sup> and a RMSE of 0.49 gC m<sup>-2</sup> d<sup>-1</sup>. It should be noted that, both the original approach as well as the coupled SOILCO2/RothC model are able to reproduce the total amount of CO<sub>2</sub> efflux for the first 5 years, which is simply a result of using this total amount in the objective function for the inversion. The measured mean respiration rate over the inversion period is 0.939 gC m<sup>-2</sup> d<sup>-1</sup>. In case of the coupled model, the inversion of the HUM decomposition rate significantly improves the agreement between simulated and measured CO<sub>2</sub> effluxes. Fig. 4a shows that the modelled soil CO<sub>2</sub> efflux is in acceptable agreement with the measurements for the coupled model (R<sup>2</sup>=0.66, IA=0.90). The MAE and the RMSE for the first 5 years are 0.23 gC m<sup>-2</sup> d<sup>-1</sup> and 0.30 gC m<sup>-2</sup> d<sup>-1</sup>, respectively. The inter-annual variations are well captured by the model, except perhaps for the second year (2000), for which the largest deviation between measured and simulated annual sums of heterotrophic respiration is detected (Table 4).

The inversion resulted in a decomposition rate constant for the humus pool of 0.04 year<sup>-1</sup> and a value of -9678 cm for h<sub>2</sub>. This decomposition rate of the HUM pool is 2.0 times higher than the original value of 0.02 year<sup>-1</sup> (Jenkinson, 1990). The original value was determined from 10 years long experiments on cropped plots. Due to root respiration, higher soil CO<sub>2</sub> con-

**Table 4 – Yearly precipitation P, ratio actual evaporation E<sub>a</sub> to potential evaporation E<sub>p</sub>, measured CO<sub>2</sub> efflux, model CO<sub>2</sub> efflux, mean absolute error MAE, root mean square error RMSE, coefficient of determination R<sup>2</sup>, Index of Agreement IA and model efficiency EF, between model and measurements**

Year	P (mm year <sup>-1</sup> )	E <sub>a</sub> /E <sub>p</sub> (-)	Measurements of CO <sub>2</sub> (gC m <sup>-2</sup> year <sup>-1</sup> )	Model CO <sub>2</sub> (gC m <sup>-2</sup> year <sup>-1</sup> )	MAE (gC m <sup>-2</sup> d <sup>-1</sup> )	RMSE (gC m <sup>-2</sup> d <sup>-1</sup> )	R <sup>2</sup>	IA	EF
1999	406.1	0.37	252.5	264.5	0.183	0.223	0.64	0.87	0.64
2000	537.5	0.49	307.3	290.7	0.184	0.234	0.44	0.79	0.36
2001	627.0	0.61	434.5	435.7	0.281	0.388	0.70	0.91	0.68
2002	762.6	0.64	335.4	333.0	0.242	0.302	0.49	0.83	0.44
2003	428.3	0.33	383.3	389.1	0.248	0.335	0.67	0.90	0.61
2004	626.3	0.60	305.8	315.1	0.183	0.229	0.72	0.92	0.70
2005	600.2	0.52	272.6	261.8	0.158	0.197	0.67	0.88	0.66
2006	502.3	0.52	221.7	255.2	0.189	0.238	0.48	0.81	0.41



**Fig. 5 – Depth/time diagrams on model results of CO<sub>2</sub> concentration, soil temperature and pressure head for the Ap horizon.**

centrations are always found for cropped plots than for bare soil, which might lead to a reduction of CO<sub>2</sub> production due to high CO<sub>2</sub> concentrations (Hashimoto and Komatsu, 2006). Since reduction according to the soil CO<sub>2</sub> concentration, as an indicator for an oxygen deficit, is not taken into account in the original RothC model (Jenkinson, 1990; Coleman and Jenkinson, 2005), it is conceivable that this partly explains the higher decomposition rate found in this study. In addition, a likely explanation for the higher inverted decomposition rate is the grubbing of the soil in order to remove the weeds. Every mechanical disturbance and destruction of soil aggregates destroys the physical protection of the humus carbon and enhances the availability of labile carbon and increases the CO<sub>2</sub> production (De Gryze et al., 2006). This higher production will lead to an increased decomposition rate in a model inversion. It should be noted that Skjemstad et al. (2001) also found a more labile RothC humus pool (decomposition rate of 0.03 year<sup>-1</sup> instead of 0.02 year<sup>-1</sup>) than originally assumed by Jenkinson (1990). However, the uncertainty associated to the inversely determined HUM pool decomposition rate constant of 0.04 year<sup>-1</sup> is rather large. For example, the sensitivity of the rate constant towards the correction of the measurements for autotrophic respiration is rather high. If no correction for autotrophic respiration would be carried out the inversely estimated decomposition rate constant for the HUM pool would be even larger and amount to 0.06 year<sup>-1</sup>, which is 2.8 times higher than the original value of Jenkinson (1990). This points at the sensitivity of the inversely estimated rate constants to the estimated autotrophic respiration.

In Fig. 5 we plotted simulated profiles of CO<sub>2</sub> concentrations and the influencing soil state variables against time. Fig. 5 shows that high CO<sub>2</sub> concentrations in the topsoil (upper 30 cm), causing high CO<sub>2</sub> effluxes, are strongly driven by soil temperature. However, also the influence of soil water content is visible in terms of the pressure head. For example, after a

dry period during the summer of 2001 ( $t=850$ ), indicated by rather high values of  $\log_{10}(h)$ , the soil respiration peaks due to a precipitation event. Apparently, the precipitation stimulated the microbial carbon decomposition, which was low because of the lack of soil water despite high soil temperatures.

Fig. 6a shows that the errors in the prediction of CO<sub>2</sub> effluxes are unbiased. There is no trend to over- or underestimate fluxes in dependence of the flux density. The deviations between measurement and model generally vary randomly around the 1:1 line. Fig. 6a also shows that the errors in the modelled CO<sub>2</sub> efflux during the inversion period are independent from the meteorological conditions, since the errors for each single year vary similarly around the 1:1 line.

In order to validate the parameters found by the model inversion, the modelled and measured CO<sub>2</sub> efflux (four parallels) of the following 3 years were analyzed. For this validation period, measurements and model are also in agreement (Fig. 7 and Table 4). The coefficient of determination for this period is 0.65 and the Index of Agreement is 0.89. The MAE and the RMSE are 0.18 and 0.22 g C m<sup>-2</sup> d<sup>-1</sup>, respectively. The measured yearly sums of CO<sub>2</sub> efflux slightly decreased from 2004 to 2006, which is well reproduced by the model, although the total amount predicted by the model for 2006 was too high (Table 4). Fig. 6b reveals that the errors between measured and simulated CO<sub>2</sub> effluxes during the 3 years of the validation period show no bias. Fig. 6b also shows that the errors during the validation period are on average as close to the 1:1 line as for the inversion period, which is further confirmed by the similar R<sup>2</sup> for the inversion and validation period. The MAE and RMSE are even smaller for the validation period.

The question arises whether the remaining discrepancies between model and measurements result from an insufficient description of the dependency of CO<sub>2</sub> production on soil temperature or on soil water content. In order to answer

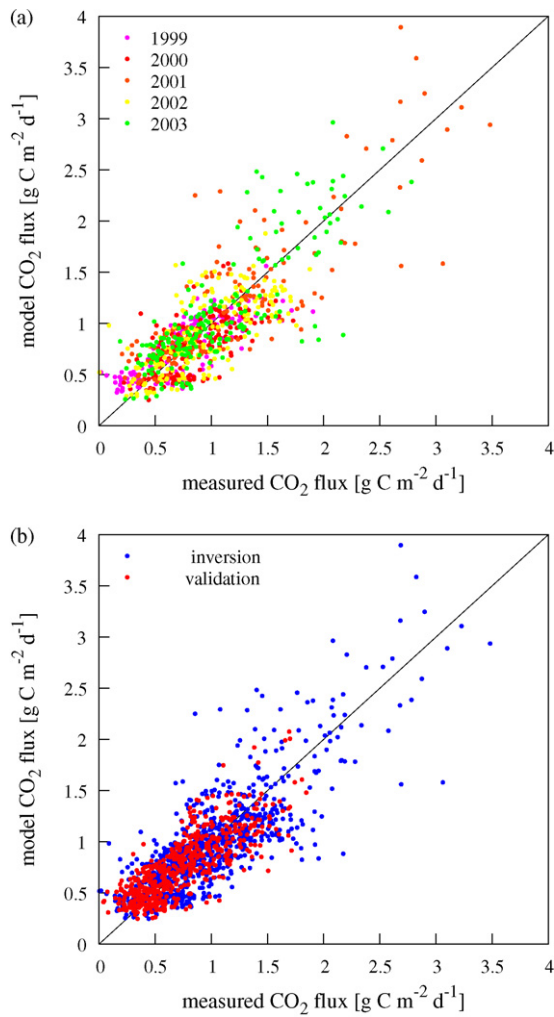


**Fig. 6 – Correlation of simulated and observed daily CO<sub>2</sub> flux for the single years of the model inversion period (a); correlation of simulated and observed daily CO<sub>2</sub> flux for the inversion and the validation period (b).**

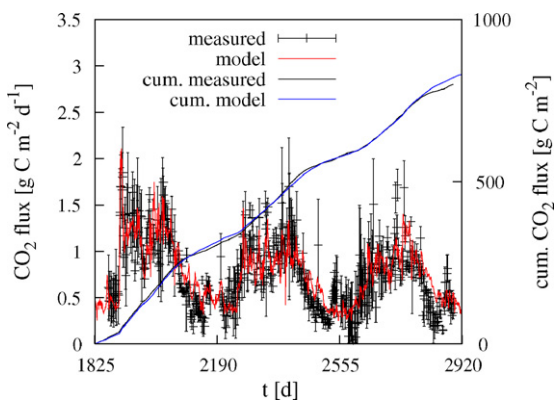


**Fig. 7 – Simulated daily fluxes, measured daily fluxes, cumulative simulated fluxes and cumulative measured fluxes of CO<sub>2</sub> for the validation period, bars indicate standard deviation of the four measurements.**

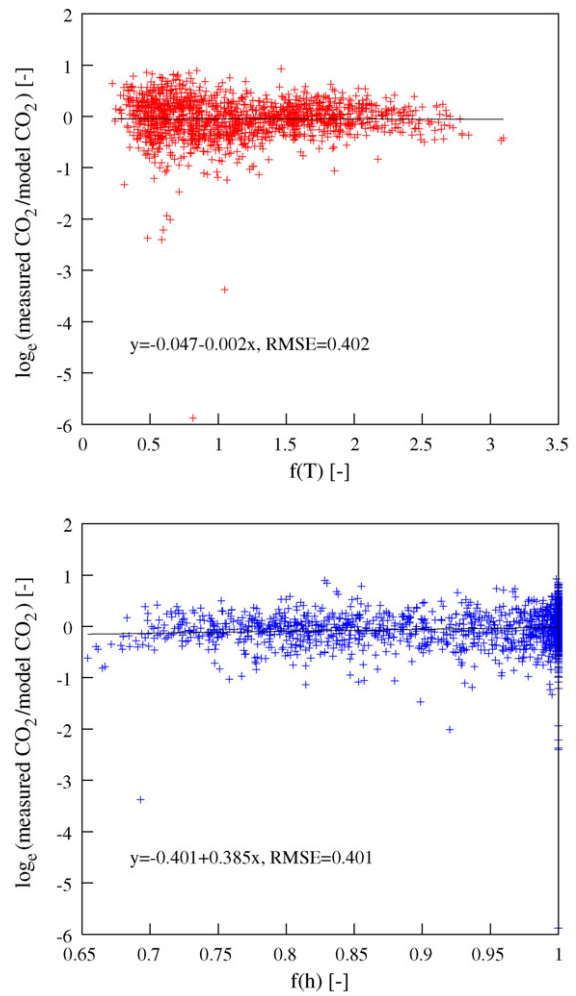


**Fig. 8 – Correlation between the ratio simulated/observed daily CO<sub>2</sub> effluxes and the estimated reduction according to temperature (top) and pressure head (bottom). The reduction factors  $f(T)$  and  $f(h)$  are average values of the upper 30 cm.**

this question, we plotted the natural logarithm of the ratio between measured and calculated CO<sub>2</sub> efflux against the reduction factors for temperature and pressure head averaged for the Ap horizon (upper 30 cm). Fig. 8 reveals that there is no temperature dependency of the deviations between measured and predicted CO<sub>2</sub> effluxes. The fitted linear regression shows an intercept very close to zero and a slope of 0.002, which is also very close to zero. For the pressure head, the intercept is also very close to zero, but there seems to be a slight bias to overestimate the CO<sub>2</sub> efflux for wet soil conditions, when  $f(h)$  is close to 1 (Fig. 8). Nevertheless, this dependency is small compared to the overall noise. The slope of the respective linear regression is 0.39, which indicates that the relation between soil water status and CO<sub>2</sub> production was probably a bigger source of errors than the relation between soil temperature and CO<sub>2</sub> production. This might also partly explain the deviations between measured and predicted CO<sub>2</sub> effluxes for 2000 (365 d < t < 730 d) and 2002 (1095 d < t < 1460 d). These results also show that soil water content is relevant

for respiration under field conditions, which corroborates the experimental findings of Akinremi et al. (1999) amongst others.

Besides potential deficits in the model, three other measurement-related factors may also contribute to the disagreement between measured and modelled daily CO<sub>2</sub> efflux. First of all, the high spatial variability of CO<sub>2</sub> efflux might play a role (Aiken et al., 1991; Rochette et al., 1991; Pringle and Lark, 2006). Fig. 7 shows that during the last 3 years (2004–2006), when four locations were sampled, a high standard deviation was detected in the measurements. Second, the temporal variability of CO<sub>2</sub> efflux might also have an influence (Dugas, 1993; Janssens et al., 2000; Nakadai et al., 2002; Tang and Baldocchi, 2005). CO<sub>2</sub> sampling was carried out during the morning for about 1 h every day. Typically, measurements during the morning give a good approximation of daily mean fluxes (Saiz et al., 2006) with a bias smaller than 5% (Parkin and Kaspar, 2004). However, in some situations the daily fluxes estimated from just 1 h might deviate from the actual daily mean (Akinremi et al., 1999). Finally, the errors in the CO<sub>2</sub> flux measurements associated with every soil respiration measurement with a chamber system probably also contributed to the disagreement between model and measurements (Janssens et al., 2000).

### 3.3. Carbon balance

Soil respiration did not decrease significantly during the eight experimental years. It was impossible to reproduce the measured temporal evolution of the CO<sub>2</sub> efflux without assuming that most of the heterotrophically respired CO<sub>2</sub> originates from the recalcitrant pools, since the 'fast' pools were rather empty and recharged only moderately from plant material input. Usually, the recalcitrant carbon stocks contribute only a minor portion to soil CO<sub>2</sub> efflux (Ryan and Law, 2005), but in our experiment about 57% of the heterotrophic CO<sub>2</sub> production originates from the decomposition of the HUM pool. The SOC content measured at the beginning of the experiment for the upper 30 cm was 3406 gC m<sup>-2</sup> (standard deviation of 599 gC m<sup>-2</sup>). The coupled model predicted a SOC content of 3081 gC m<sup>-2</sup> at the end of the experiment, equivalent to a loss of 10%. The SOC content measured at the end of the experiment was 3025 gC m<sup>-2</sup> (standard deviation of 375 gC m<sup>-2</sup>). Fig. 9 shows that the simulation results for the topsoil are close to the measured SOC content. The simulated SOC content for the soil horizon below (30–60 cm depth) was also in good agreement with the measured SOC content at the end of the experiment. Unfortunately, no measurements were available for the SOC content of the deeper soil layers at the start of the experiment. In the model, the initial SOC content of the entire soil profile was assumed to be 6724 gC m<sup>-2</sup>. At the end of the experiment, the simulated SOC content was 5546 gC m<sup>-2</sup>, equivalent to a loss of 18%. This soil carbon loss of 1178 gC m<sup>-2</sup> is accompanied by a heterotrophic CO<sub>2</sub>-C emission of 2516 gC m<sup>-2</sup> (measured: 2513 gC m<sup>-2</sup>). The gap is explained by the input of fresh plant material, which was accounted for by assuming a rather small carbon input from plant material of 177 gC m<sup>-2</sup> year<sup>-1</sup>.

In general, it should be noted that it is rather difficult to validate the carbon turnover in the model for this experiment,

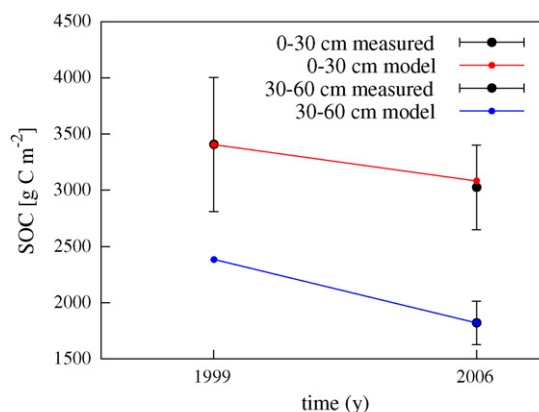


**Fig. 9 – Simulated and measured soil organic carbon (SOC) contents at the beginning and at the end of the model period, bars indicate standard deviation of the measurements.**

since the loss of carbon over the 8 years is rather small compared to the accuracy of the measurements. In general the measurements seem to support the trends predicted by the model (Fig. 9). However, it should be remembered that the carbon balance was also used to initialize the model with respect to soil organic content of the deeper soil layers and the input of fresh plant material, which means that the results presented in Fig. 9 cannot be considered as an independent validation. In addition, the inverse determination of the HUM pool decomposition rate constant from this experiment is uncertain because of the unknown SOC contents in the subsoil layer, the accuracy of the SOC measurements, the unknown parameter  $h_2$  of the soil water content reduction function and the unknown amount of fresh plant material. For example, the latter has a big influence on the carbon balance of the topsoil (0–30 cm). Assuming that no input of fresh plant material occurred leads to a relative carbon loss of 23% instead of the finally simulated loss of 10%, which is quite close to the measured value of 11%. Scaling the amount of fresh plant material reveals the sensitivity of topsoil carbon loss to this input variable. Scaling factors of 0.5, 1.5 and 2.0 applied to the amount of fresh plant material lead to topsoil carbon losses of 17, 4.4 and –1.9%. The latter indicates even an increase of topsoil carbon content. This points to the fact, that for any experimental setup in terms of carbon balancing the input of carbon from fresh plant material should be determined as accurately as possible.

## 4. Summary and conclusions

The comparison between the original SOILCO<sub>2</sub> and the coupled SOILCO<sub>2</sub>/RothC revealed a significant improvement of the CO<sub>2</sub> efflux estimation with the coupled model presented in this study. The coupled model shows an improved  $R^2$  of 0.66 compared to the original SOILCO<sub>2</sub> with an  $R^2$  of 0.18. The model inversion with the coupled model for the first 5 years allows the accurate prediction of CO<sub>2</sub> efflux for the following 3 years. Against the background of the use of literature

values and pedotransfer functions for the model parameterisation, the overall model performance is acceptable. The model was able to predict the inter-annual variability of CO<sub>2</sub> efflux well. Thus, the coupling concept is seen as a promising tool to describe the heterotrophic part of the carbon cycle in soils from the input of plant residues to the release as CO<sub>2</sub>.

The calibration of the HUM pool decomposition rate constant revealed that it is possible to determine a 'slow' carbon pool decomposition rate constant from long-term soil respiration measurements under field conditions. The inversely determined value of 0.04 year<sup>-1</sup> is higher than the one suggested by the model developers, which is mainly attributed to the agricultural practice during this experiment. The uncertainty in the inversion of the HUM pool decomposition rate constant mainly arises from the initial organic carbon contents, the unknown amount of input from fresh plant material and the unknown parameter  $h_2$  of the soil water content reduction function.

## REFERENCES

- Aiken, R.M., Jawson, M.D., Grahammer, K., Polymenopoulos, A.D., 1991. Positional, spatially correlated and random components of variability in carbon dioxide efflux. *J. Environ. Qual.* 20, 301–308.
- Akinremi, O.O., McGinn, S.M., McLean, H.D., 1999. Effects of soil temperature and moisture on soil respiration in barley and fallow plots. *Can. J. Soil Sci.* 79, 5–13.
- Andrén, O., Paustian, K., 1987. Barley straw decomposition in the field: a comparison of models. *Ecology* 68, 1190–1200.
- Cannavo, P., Lafolie, F., Nicolardot, B., Renault, P., 2006. Modeling seasonal variations in carbon dioxide and nitrous oxide in the vadose zone. *Vadose Zone J.* 5, 990–1004, doi:10.2136/vzj2005.0124.
- Coleman, K., Jenkinson, D.S., 2005. RothC-26.3. A Model for Turnover of Carbon in Soil, Model Description and Windows Users Guide. IACR-Rothamsted, Harpenden, 45 pp. <http://www.rothamsted.bbsrc.ac.uk/aen/carbon/rothc.htm>.
- Cook, F.J., Thomas, S.M., Kelliher, F.M., Whitehead, D., 1998. A model of one-dimensional steady-state carbon dioxide diffusion from soil. *Ecol. Model.* 109, 155–164.
- Davidson, E.A., Janssens, I.A., 2006. Temperature sensitivity of soil carbon decomposition and feedbacks to climate change. *Nature* 440, 165–173, doi:10.1038/nature04514.
- De Gryze, S., Six, J., Merckx, R., 2006. Quantifying water stable soil aggregate turnover and its implication for soil organic matter dynamics in a model study. *Eur. J. Soil Sci.* 57, 693–707, doi:10.1111/j.1365-2389.2005.00760.x.
- Dugas, W.A., 1993. Micrometeorological and chamber measurements of CO<sub>2</sub> flux from bare soil. *Agric. For. Meteorol.* 67, 115–128.
- Eliasson, P.E., McMurtrie, R.E., Pepper, D.A., Strömberg, M., Linder, S., Ågren, G.I., 2005. The response of heterotrophic CO<sub>2</sub> flux to soil warming. *Global Change Biol.* 11, 167–181, doi:10.1111/j.1365-2486.2004.00878.x.
- Falloon, P., Smith, P., Coleman, K., Marshal, S., 1998. Estimating the size of the inert organic matter pool from total soil organic carbon content for use in the Rothamsted carbon model. *Soil Biol. Biochem.* 30 (8/9), 1207–1211.
- Fang, C., Moncrieff, J.B., 1999. A model for soil CO<sub>2</sub> production and transport. 1: Model development. *Agric. For. Meteorol.* 95, 225–236.
- Fang, C., Moncrieff, J.B., 2001. The dependence of soil CO<sub>2</sub> efflux on temperature. *Soil Biol. Biochem.* 33, 155–165.
- Franko, U., Crocker, G.J., Grace, P.R., Klír, J., Körschens, M., Poulton, P.R., Richter, D.D., 1997. Simulating trends in soil organic carbon in long-term experiments using the candy model. *Geoderma* 81, 109–120.
- Garnier, P., Néel, C., Aita, C., Recous, S., Lafolie, F., Mary, B., 2003. Modelling carbon and nitrogen dynamics in a bare soil. *Eur. J. Soil Sci.* 54, 1–14.
- Hashimoto, S., Komatsu, H., 2006. Relationships between soil CO<sub>2</sub> concentration and CO<sub>2</sub> production, temperature, water content, and gas diffusivity: implications for field studies through sensitivity analyses. *J. For. Res.* 11, 41–50.
- Hellebrand, H.J., Kern, J., Scholz, V., 2003. Long-term studies on greenhouse gas fluxes during cultivation of energy crops on sandy soils. *Atmos. Environ.* 37, 1635–1644.
- Hellebrand, H.J., Kalk, W.-D., Scholz, V., 2005. Kohlenstoffdioxid- und Methanflußraten sandiger Böden. In: Weigel, H.-J., Dämmgen, U. (Eds.), *Biologische Senken für atmosphärischen Kohlenstoff. Landbauforschung Völkenrode SH 280*, pp. 121–130.
- IPCC, 2007. *Climate Change 2007: The Physical Science Basis. Summary for Policymakers*. 18 pp.
- Janssens, I.A., Kowalski, A.S., Longdoz, B., Ceulemans, R., 2000. Assessing forest soil CO<sub>2</sub> efflux: an in situ comparison of four techniques. *Tree Physiol.* 20, 23–32.
- Jassal, R.S., Black, T.A., Drewitt, G.B., Novak, M.D., Gaumont-Guay, D., Nescic, Z., 2004. A model of the production and transport of CO<sub>2</sub> in soil: predicting soil CO<sub>2</sub> concentrations and CO<sub>2</sub> efflux from a forest floor. *Agric. For. Meteorol.* 124, 219–236.
- Jenkinson, D.S., 1990. The turnover of organic carbon and nitrogen in soil. *Phil. Trans. R. Soc. Lond. B* 329, 361–368.
- Kirschbaum, M.U.F., Eamus, D., Gifford, R.M., Roxburgh, S.H., Sands, P.J., 2001. Definitions of some ecological terms commonly used in carbon accounting. In: Kirschbaum, M.U.F., Mueller, R. (Eds.), *Net Ecosystem Exchange, Workshop Proceedings, Cooperative Research Centre for Greenhouse Accounting, April 2001, Australia*, pp. 1–5. <http://www.greenhouse.crc.org.au/crc/ecarbon/publications/nee/nee2001.htm>.
- Molina, J.-A., Smith, P., 1998. Modelling carbon and nitrogen processes in soils. *Adv. Agron.* 62, 253–298.
- Nakadai, T., Yokozawa, M., Ikeda, H., Koizumi, H., 2002. Diurnal changes of carbon dioxide flux from bare soil in agricultural field in Japan. *Appl. Soil Ecol.* 19, 161–171.
- Nash, J.E., Sutcliffe, J.V., 1970. River flow forecasting through conceptual models. Part I. A discussion of principles. *J. Hydrol.* 10, 282–290.
- Nelder, J.A., Mead, R.A., 1965. A simplex method for function minimization. *Comput. J.* 7, 308–313.
- Parkin, T.B., Kaspar, T.C., 2004. Temporal variability of soil carbon dioxide flux: effect of sampling frequency on cumulative carbon loss estimation. *Soil Sci. Soc. Am. J.* 68, 1234–1241.
- Parton, W.J., Pulliam, W.M., Ojima, D.S., 1994. Application of the CENTURY model across the LTR network: parameterization and climate change simulations. *Bull. Ecol. Soc. Am.* 75, 186–187.
- Paustian, K., Six, J., Elliott, E.T., Hunt, H.W., 2000. Management options for reducing CO<sub>2</sub> emissions from agricultural soils. *Biogeochemistry* 48, 147–163.
- Penman, H.L., 1948. Natural evaporation from open water, bare soil and grass. *Proceedings of the Royal Society of London, Series A—Mathematical and Physical Sciences* 193, 120–145.
- Pringle, M.J., Lark, R.M., 2006. Spatial analysis of model error, illustrated by soil carbon dioxide emissions. *Vadose Zone J.* 5, 168–183, doi:10.2136/vzj2005.0015.
- Pumpanen, J., Ilvesniemi, H., Hari, P., 2003. A process-based model for predicting soil carbon dioxide efflux and concentration. *Soil Sci. Soc. Am. J.* 67, 402–413.

- Rawls, W., Brakensiek, D.L., 1985. Prediction of soil water properties for hydrologic modelling. *Am. Soc. Civil Eng.*, 293–299.
- Rochette, P., Desjardins, R.L., Pattey, E., 1991. Spatial and temporal variability of soil respiration in agricultural fields. *Can. J. Soil Sci.* 71, 189–196.
- Rodrigo, A., Recous, S., Neel, C., Mary, B., 1997. Modelling temperature and moisture effects on C–N transformations in soils: comparison of nine models. *Ecol. Model.* 102, 325–339.
- Ryan, M.G., Law, B.E., 2005. Interpreting, measuring, and modelling soil respiration. *Biogeochemistry* 73, 3–27.
- Saiz, G., Byrne, K.A., Butterbach-Bahl, K., Kiese, R., Blujdea, V., Farrell, E.P., 2006. Stand age-related effects on soil respiration in a first rotation Sitka spruce chronosequence in central Ireland. *Global Change Biol.* 12, 1–14, doi:10.1111/j.1365-2486.2006.01145.x.
- Scott-Denton, L.E., Rosenstiel, T.N., Monson, R.K., 2006. Differential controls by climate and substrate over the heterotrophic and rhizospheric components of soil respiration. *Global Change Biol.* 12, 205–216, doi:10.1111/j.1365-2486.2005.01064.x.
- Šimůnek, J., Suarez, D.L., 1993. Modeling of Carbon dioxide transport and production in soil. 1. Model development. *Water Resources Res.* 29 (2), 487–497.
- Šimůnek, J., Suarez, D.L., Sejna, M., 1996. The UNSATCHEM software package for simulating the one-dimensional variably saturated water flow, heat transport, carbon dioxide production and transport, and multicomponent solute transport with major ion equilibrium and kinetic chemistry. Version 2.0. USSL Report No. 141, Riverside, California.
- Skjemstad, J.O., Dalal, R.C., Janik, L.J., McGowan, J.A., 2001. Changes in chemical nature of soil organic carbon in vertisols under wheat in south-eastern Queensland. *Aust. J. Soil Res.* 39 (2), 343–359.
- Skjemstad, J.O., Spouncer, L.R., Cowie, B., Swift, R.S., 2004. Calibration of the Rothamsted organic carbon turnover model (RothC ver. 26.3), using measurable soil organic pools. *Aust. J. Soil Res.* 42, 79–88.
- Smith, M., Allen, R., Pereira, L., 1996. Revised FAO methodology for crop water requirements. FAO-Report. 10 pp.
- Smith, P., Smith, J.U., Powlson, D.S., McGill, W.B., Arah, J.R.M., Chertov, O.G., Coleman, K., Franko, U., Frolking, S., Jenkinson, D.S., Jensen, L.S., Kelly, R.H., Klein-Gunnewiek, H., Komarov, A.S., Li, C., Molina, J.A.E., Mueller, T., Parton, W.J., Thornley, J.H.M., Whitmore, A.P., 1997. A comparison of the performance of nine soil organic matter models using datasets from seven long-term experiments. *Geoderma* 81, 153–225.
- Smith, K.A., Ball, T., Conen, F., Dobbie, K.E., Massheder, J., Rey, A., 2003. Exchange of greenhouse gases between soil and atmosphere: interactions of soil physical factors and biological processes. *Eur. J. Soil Sci.* 54, 779–791.
- Suwa, M., Katul, G.G., Oren, R., Andrews, J., Phippen, J., Mace, A., Schlesinger, W.H., 2004. Impact of elevated atmospheric CO<sub>2</sub> on forest floor respiration in a temperate pine forest. *Global Biogeochem. Cycles* 18, GB2013, doi:10.1029/2003GB002182.
- Tang, J., Baldocchi, D.B., 2005. Spatial-temporal variation in soil respiration in an oak-grass savanna ecosystem in California and its partitioning into autotrophic and heterotrophic components. *Biogeochemistry* 73, 183–207.
- Trumbore, S., 2006. Carbon respired by terrestrial ecosystems—recent progress and challenges. *Global Change Biol.* 12, 141–153, doi:10.1111/j.1365-2486.2005.01067.x.
- Van Genuchten, M.Th., 1980. A closed form equation for predicting the hydraulic conductivity of unsaturated soils. *Soil Sci. Soc. Am. J.* 44, 892–898.
- Willmott, C.J., 1981. On the validation of models. *Phys. Geogr.* 2, 184–194.
- Zak, D.R., Holmes, W.E., MacDonald, N.W., Pregitzer, K.S., 1999. Soil temperature, matric potential, and the kinetics of microbial respiration and nitrogen mineralization. *Soil Sci. Soc. Am. J.* 63, 575–584.
- Zimmermann, M., Leifeld, J., Schmid, M.W.I., Smith, P., Fuhrer, J., 2007. Measured soil organic matter fractions can be related to pools in the RothC model. *Eur. J. Soil Sci.* 58, 658–667, doi:10.1111/j.1365-2389.2006.00855.x.